Direct Evidence of Flux Cutting in Type-II Superconductors

G. Fillion, R. Gauthier, and M. A. R. LeBlanc
Physics Department, University of Ottawa, Ottawa K1N6N5, Canada
(Received 13 March 1979)

A hollow cylinder of a hysteretic type-II superconductor allows applied axial flux to enter the hole smoothly while sustaining trapped azimuthal flux until H_{c2} is attained showing clearly that flux cutting occurs. A comparison of the evolution of the axial flux, with and without trapped azimuthal flux in the wall, yields data on the energy associated with flux-cutting events. Our technique lends itself to a study of the role of many pertinent parameters in this phenomenon.

In 1972, Walmsley[1] and also Campbell and Evetts[2] put forward the concept of flux cutting. According to this idea, adjacent flux lines, initially twisted or tilted, can intersect and reform in such a manner that there are no free ends within the volume of the superconductor. This mechanism has been invoked to account for a variety of phenomena encountered when wires of type-II superconductors are carrying a transport current while immersed in a longitudinal magnetic field. In particular, the process is useful in explaining the observation, under these circumstances, of (i) steady flux-flow voltages above I_c accompanied by a steady axial moment[1-7] and (ii) coupled resistive and magnetic oscillations at frequencies in the kilohertz range.[6] Flux cutting also presumably plays a role in the occurrence of complex electric potential structure on the surface of the wires.[8-10] Powerful evidence for flux cutting has been provided by the measurements of Cave, Evetts, and Campbell,[11] which reveal that under ac conditions the quantity of azimuthal flux entering and leaving the specimen is conserably in excess of the movement of axial flux. The empirical equation exploited by Gauthier and LeBlanc[12] to describe the spatial variation of the helical sheets of flux lines in their calculation of ac losses implies that flux cutting occurs. Clem[13] examines in detail a dynamical double-helix configuration involving flux-cutting events to explain steady longitudinal voltages with stationary magnetization.

In this article we report on an experiment which, in our view, provides unambiguous evidence for the occurrence of flux cutting. First, azimuthal flux is trapped in the wall of a hollow type-II superconducting cylinder. The wall is subsequently observed to retain an appreciable fraction of this trapped flux until H_{c2} is attained while flux threading the hole is seen to increase smoothly from zero to H_{c2} as an externally applied longitudinal magnetic field is imposed. These measurements show that orthogonal sheets of flux lines do indeed cross through each other. Further, our data yield estimates of the energy involved in flux-cutting events. Our approach provides a technique for studying the role of various parameters, such as pinning strength, thermodynamic critical field, flux density, and relative orientation of flux sheets, etc., on the flux-cutting energy.

The sample assembly comprises the following concentric components enumerated and described in their radial sequence (see Fig. 1).

(a) A 15-cm-long straight wire of 0.025-cm-diam NbTi core which is used to provide the azimuthal magnetic induction $B_\theta = \mu_0 I/2\pi r$, where I is the transport current fed through the wire. Two rigidly mounted massive copper blocks are pressed on the ends of this wire. (b) An inner pickup coil (3.8 cm long, 20 000 turns) monitors B_i, the longitudinal magnetic induction in the hole of the tube. (c) A vanadium (metallurgical-grade) tube sample, 10 cm in length, 0.660 cm o.d. with a 0.017-cm-thick wall. (d) A noninductively (bifilar) wound single-layer, 0.010-cm-diam Manganin wire heater coil snugly embracing the entire length of the sample. (e) A toroidal pickup coil of 1200 turns embracing the wall of the tube sample monitors $\langle B_\theta \rangle$, the average azumuthal magnetic induction in this volume. (f) An outer pickup coil. This pickup coil is 5.7 cm long, 2.5 cm o.d. and 1.3 cm i.d., and consists

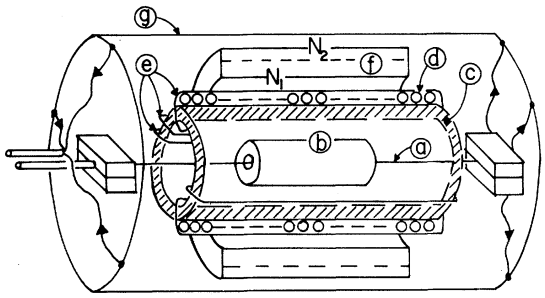

FIG. 1. Sample assembly. (a)–(g) As in the text. Superconducting solenoid not shown.

of two concentric coils connected in series opposition. Since we have adjusted $N_1\langle A_1\rangle \simeq N_2\langle A_2\rangle$, where N_1 and N_2 are the number of turns and $\langle A_1\rangle$ and $\langle A_2\rangle$ are the average circular areas of each coil, the total coil is balanced against a uniform longitudinal magnetic field but can detect the magnetization of the sample since $N_1 - N_2 \approx 60\,000$. (g) A copper tube which serves as a return path for the current I fed to the NbTi wire. The base of this cylinder is electrically connected by a symmetric array of leads to the lower copper block. One of a twisted pair of heavy insulated copper leads from the external current source is similarly attached to the top of this cylinder while the other is directly connected to the upper copper block. (h) A superconducting solenoid, 16.5 cm long, 3.8 cm i.d., and 5.7 cm o.d., provides the longitudinal magnetic field $H_\parallel$.

The inner, the toroidal, and the outer pickup coils feed each an electronic amplifier-integrator driving the y axes of three separate x-y recorders. A signal proportional to $H_\parallel$, the magnetic field of the solenoid, simultaneously drives the x axes of these recorders. Consequently, as $H_\parallel$ is increased we continuously monitor B_i, $\langle B_\theta\rangle$, and $\langle M_z\rangle$, the magnetization of the sample cylinder versus $H_\parallel$.

With $H_\parallel = 0$ and a steady current flowing in the NbTi wire, the vanadium tube is heated above T_c and subsequently allowed to cool to or nearly to the ambient 4.2-K helium-bath temperature. No expulsion of azimuthal flux is observed during cooling. The current I, typically ≈ 320 A in our work, is then reduced to zero. The wall of the tube appears to retain all of the azimuthal flux initially threading it.

With no trapped azimuthal flux and the sample at 4.2 K, unless the increase of $H_\parallel$ proceeds smoothly and slowly, a flux jump can be triggered near the summit of the diamagnetic magnetization curve causing B_i to rise abruptly. For this reason we have found it useful to operate at a temperature slightly above 4.2 K ($T \approx 4.4$ K) where this problem vanishes. In the data exemplified by

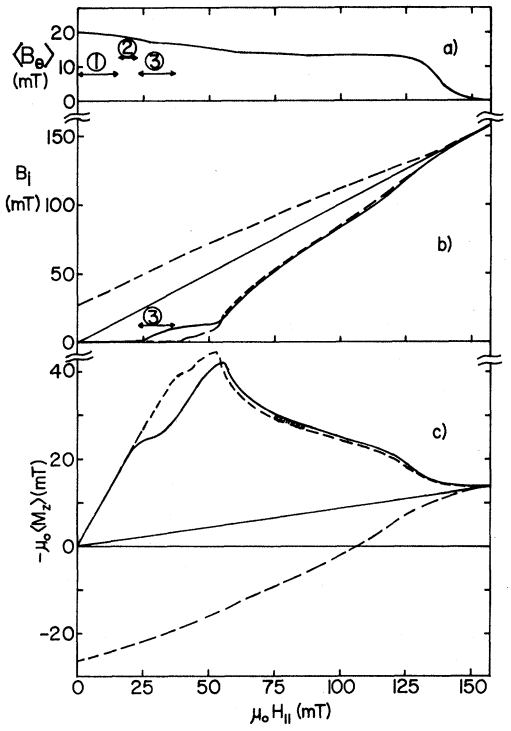

FIG. 2. (a) Evolution of average trapped azimuthal magnetic induction $\langle B_\theta\rangle$ vs $H_\parallel$. (b) Evolution of the axial magnetic induction B_i with trapped azimuthal flux (solid) and without (dashed curve). (c) Evolution of the axial magnetization $\langle M_z\rangle$ of the hollow cylinder (wall plus hole) vs $H_\parallel$ with trapped azimuthal flux (solid) and without (dashed curves). Normal-state base line is tilted from the horizontal because of imperfect balancing of the pickup coil. $T \approx 4.4$ K. Data for (a), (b), and (c) were taken simultaneously.

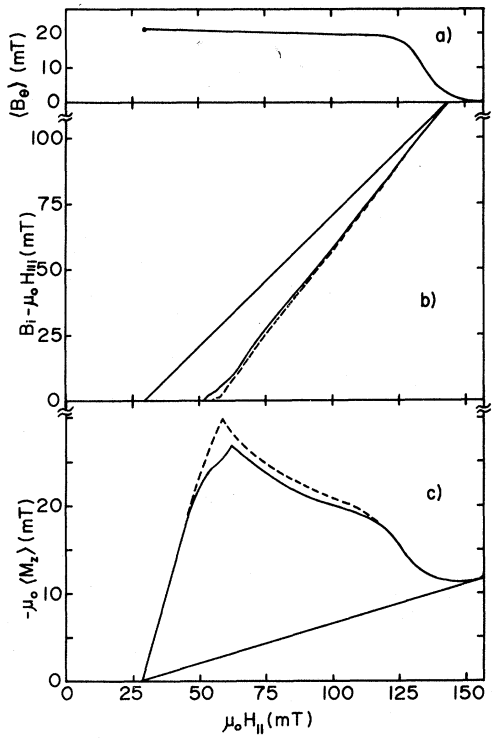

FIG. 3. As in Fig. 2 but here $\mu_0 H_{\parallel i} = 28.5$ mT instead of zero and in (b) we show $B_i - \mu_0 H_{\parallel i}$ vs $H_\parallel$, where 45° line is normal-state curve.

Figs. 2 and 3, there is no evidence that the mechanism of flux jumping is playing a role in the process of flux penetration since the pen tracings are smooth and continuous. We did not encounter the problem of flux jumps with azimuthal flux trapped in the wall. This stability appears to be related to the fact that, under these circumstances, the gradual entry of axial flux in the hole now begins at a significantly smaller $H_{\parallel}$.

In Fig. 2 we display a typical set of tracings of the evolution of $\langle M_z \rangle$, B_i, and $\langle B_\theta \rangle$ as $H_{\parallel}$ is applied with and without trapped azimuthal flux (solid and dashed curves, respectively). The most dramatic feature which emerges from inspection of these data curves is that a substantial fraction of the azimuthal flux, φ_θ, initially trapped in the wall of the sample survives till near H_{c2} while axial flux smoothly penetrates into the hollow of the tube.

Further, we note that, beyond the summits in $\langle M_z \rangle$, the internal field B_i at corresponding $H_{\parallel}$ is weaker ($|\langle M_z \rangle|$ is larger) when azimuthal flux is trapped compared with the situation where $\varphi_\theta = 0$. We conclude that, here, the azimuthal flux-line lattice aids the pinning forces in opposing the penetration of the longitudinal flux into the hole. From the separation between the $\langle M_z \rangle$ curves we can estimate the energy dissipated (liberated) per flux cutting event. An increment, ΔB_i, of axial flux density means that $\Delta N = (\Delta B_i)\pi R_i^2/\varphi_0$ flux lines have entered the hole. Each of these flux lines has crossed through $n = \langle B_\theta \rangle (R_0 - R_i) l/\varphi_0$ azimuthal flux lines where φ_0 is the flux quantum, R_i, R_0, and l are, respectively, the inner radius, outer radius, and length of the hollow cylinder. When φ_0 is constant over an increment $\Delta H_{\parallel}$, the energy difference, ΔU, associated with the $n\,\Delta N$ flux cutting events can be written

$$\Delta U = V\left(\int H_{\parallel}'\, d\langle B_z' \rangle - \int H_{\parallel}\, d\langle B_z \rangle\right), \tag{1}$$

where the prime indicates the situation where $\varphi_\theta \neq 0$. Here $V = \pi R_0^2 l$ (ignoring end effects). $\langle B_z' \rangle$ and $\langle B_z \rangle$, the average axial magnetic induction in the tube (wall plus hole) spans the same range in both integrals. When $\langle M_z' \rangle$ and $\langle M_z \rangle$ vs $H_{\parallel}$ are nearly parallel (and φ_θ constant), ΔU, represented by the shaded area in the $\langle M \rangle$-H plane [see Fig. 2(c)] is approximately given by

$$\Delta U \approx \mu_0(\langle M_z \rangle - \langle M_z' \rangle)(\Delta H_{\parallel})V\,. \tag{2}$$

The energy $\epsilon = n^{-1}\Delta U/\Delta N$, per flux-cutting event, is then given by

$$\epsilon \approx \frac{\mu_0(\langle M_z \rangle - \langle M_z' \rangle)(\Delta H_{\parallel})\varphi_0^2 R_0^2}{\langle B_\theta \rangle (\Delta B_i)(R_0 - R_i)R_i^2}\,. \tag{3}$$

From Fig. 1 we obtain $\epsilon \approx 1.2 \times 10^{-21}$ J event where we have taken $\mu_0(\langle M_z \rangle - \langle M_z' \rangle) \approx 1.2$ mT, $\mu_0 H_{\parallel}/\Delta B_i \approx 0.7$, and $\langle B_\theta \rangle \approx 15$ mT.

In Fig. 2, the longitudinal flux lines entering the outer surface and crossing the inner surface are orthogonal to the lattice of trapped azimuthal flux. This special configuration was chosen as an ideal situation for testing the concept of flux cutting. If we now relax the condition that the interpenetrating flux lattices be orthogonal, our experimental setup readily lends itself to a study of the dependence of flux cutting on the angle α between the intersecting flux lines. We prepare a helical flux-line lattice by allowing the tube to become superconducting in a selected stationary combination of B_θ and $H_{\parallel}$ (denoted $H_{\parallel i}$). This lattice is trapped essentially undistrubed when I is removed. Subsequently increasing (or decreasing) $H_{\parallel}$ causes longitudinal flux to migrate through this helical lattice into (or out of) the hole. Figure 3 shows typical behavior for $H_{\parallel}$ increasing. Here the initial $\alpha = \tan^{-1} I/2\pi R H_{\parallel i} \approx 30°$, where $R_i \leq R \leq R_0$. We note that the relative position of the B_i and $\langle M_z \rangle$ curves are reversed from that in Fig. 1, hence ϵ is now negative. A discussion of the behavior of ϵ is beyond the scope of this Letter and its variation with α is under study.

Our interpretation of the complicated behavior before the summits of $\langle M_z \rangle$ vs $H_{\parallel}$ are reached is not crucial for the above analysis. It is sufficient, here, to indicate that, from our data, we visualize the following sequence of events (see Fig. 2). Perfect shielding against $H_{\parallel}$ but leakage of φ_0 through the outer surface (region 1, $0 \lesssim \mu_0 H_{\parallel} \lesssim 15$ mT). Penetration of axial flux into the wall accompanied by a further exit of azimuthal flux, the decrease of the magnetic energy stored in the B_θ profile contributing to the flux-cutting processes which are occurring (region 2, 15 mT $\lesssim \mu_0 H_{\parallel} \lesssim$ 22 mT). The difference between the applied fields for entry of axial flux into the hole with ($H_{\parallel}' \approx 22$ mT) and without ($H_{\parallel}'' \approx 37$ mT) trapped azimuthal flux is a measure of the inner surface barrier of the tube (region 3). The behavior in the range 37 mT $\lesssim \mu_0 H_{\parallel} \lesssim$ 52 mT, with and without φ_θ, is perplexing. We may invoke end effects to account for the phenomena here but this explanation is not entirely satisfactory. Beyond the peaks in $\langle M_z \rangle$, the critical bulk and surface currents decline with increasing $H_{\parallel}$, hence $\Delta B_i/\mu_0 H_{\parallel} > 1$.

Our observations of the smooth penetration of axial flux in the hole of a type-II superconducting tube as an axial magnetic field $H_{\parallel}$ is imposed, while the wall of the tube sustains trapped azimuthal flux, conclusively demonstrate the phenomenon of flux cutting. The differences in the data curves, with and without azimuthal flux trapped in the wall, are exploited to determine the energy ϵ associated with flux cutting. We find that ϵ is positive when the trapped flux is purely azimuthal but becomes negative when the longitudinal flux is made to traverse helical configurations of flux trapped in the wall. This dependence of flux cutting on the relative orientation of the intersecting flux lines and on other parameters is under active study with use of the simple technique which we have described.

We are indebted to Dr. J. F. Bussière of Brookhaven National Laboratory for supplying the vanadium tube and Dr. J. R. Cave of this laboratory for a useful discussion of flux cutting.

[1]D. G. Walmsley, J. Phys. F 2, 510 (1972).
[2]A. M. Campbell and J. E. Evetts, Adv. Phys. 21, 199 (1972).
[3]D. G. Walmsley and W. E. Timms, J. Phys. F 3, L203 (1973).
[4]W. E. Timms and D. G. Walmsley, J. Phys. F 5, 287 (1975).
[5]W. E. Timms and D. G. Walmsley, J. Phys. F 6, 2107 (1976).
[6]D. G. Walmsley and W. E. Timms, J. Phys. F 7, 2373 (1977).
[7]J. E. Nicholson and P. T. Sikora, J. Low Temp. Phys. 17, 275 (1974).
[8]F. Irie, T. Ezaki, and K. Yamafuji, IEEE Trans. Mag. 11, 332 (1975).
[9]T. Ezaki and F. Irie, J. Phys. Soc. Jpn. 40, 382 (1976).
[10]J. R. Cave and J. E. Evetts, Philos. Mag. B37, 111, 663(E) (1978).
[11]J. R. Cave, J. E. Evetts, and A. M. Campbell, J. Phys. (Paris), Colloq. 39, C6-614 (1978).
[12]R. Gauthier and M. A. R. LeBlanc, IEEE Trans. Mag. 13, 560 (1977).
[13]J. R. Clem, Phys. Rev. Lett. 38, 1425 (1977).

ERRATA

SPECIFIC-HEAT ANOMALIES AT THE LOWER CRITICAL TEMPERATURE IN REENTRANT FERROMAGNETIC SUPERCONDUCTORS. H. B. MacKay, L. D. Woolf, M. B. Maple, and D. C. Johnston [Phys. Rev. Lett. 42, 918 (1979)].

Figure 3 was in error and should be replaced by the corrected figure which is shown here. The error does not change any of the statements or conclusions in the article.

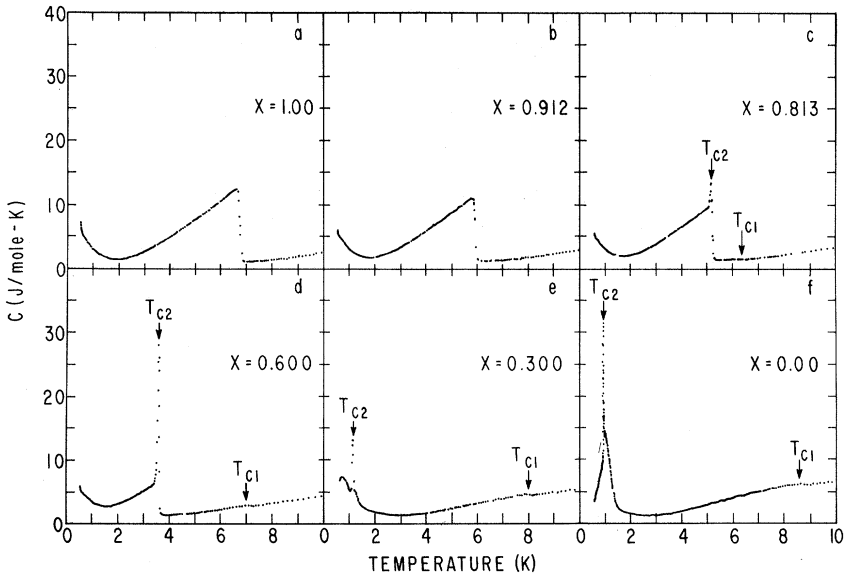

FIG. 3. Heat capacity C vs temperature for certain members of the $(Er_{1-x}Ho_x)Rh_4B_4$ system. The arrows indicate the upper (T_{c1}) and lower (T_{c2}) SC-N transition temperatures as measured by ac magnetic susceptibility.